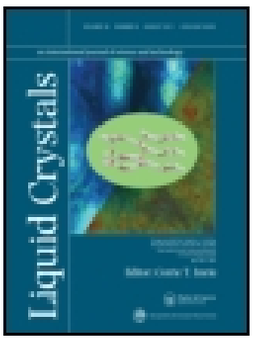

Liquid Crystals

ISSN: 0267-8292 (Print) 1366-5855 (Online) Journal homepage: https://www.tandfonline.com/loi/tlct20

Nuclear magnetic resonance studies of translational diffusion in thermotropic ionic liquid crystals

Sergey V. Dvinskikh

To cite this article: Sergey V. Dvinskikh (2019): Nuclear magnetic resonance studies of translational diffusion in thermotropic ionic liquid crystals, Liquid Crystals, DOI: 10.1080/02678292.2019.1647569

To link to this article: https://doi.org/10.1080/02678292.2019.1647569

Published online: 31 Jul 2019.

LIQUID CRYSTALS
https://doi.org/10.1080/02678292.2019.1647569

Taylor & Francis
Taylor & Francis Group

Nuclear magnetic resonance studies of translational diffusion in thermotropic ionic liquid crystals

Sergey V. Dvinskikh

Department of Chemistry, KTH Royal Institute of Technology, Stockholm, Sweden; Laboratory of Biomolecular NMR, Saint Petersburg State University, Saint Petersburg, Russia

ABSTRACT

The NMR methodologies employed for investigating translational diffusion in anisotropic fluids and the results of their applications to ionic liquid crystals are reviewed. Experiments on ionic liquid crystals are preferably performed using oriented samples and require magnetic field gradients in orthogonal directions. Diffusion experiments in anisotropic systems with broad NMR lines are performed using line narrowing techniques and by application of strong static or pulsed field gradients for efficient gradient encoding/decoding of the spatial locations of molecules. Self-diffusion studies on various thermotropic ion-conductive materials exhibiting smectic, cubic, and columnar phases have been reported. Diffusion rates and anisotropy characterise the translational dynamics of ions in nanostructures and reflect the molecular ordering and ion pairing/dissociation processes. Distinct diffusion behaviours were observed for cations and anions. The knowledge of molecular mobility in ionic liquid crystals is important for the understanding their dynamic properties and is, therefore, valuable for the development of anisotropic soft materials for ion transport.

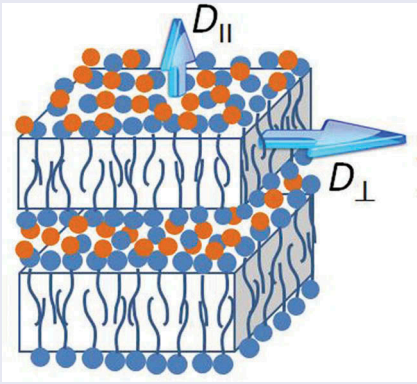

ARTICLE HISTORY
Received 17 April 2019
Accepted 21 July 2019

KEYWORDS
Ionic liquid crystals; smectic; columnar; cubic; anisotropic translational diffusion; pulsed-field-gradient NMR

1. Introduction

Organic salts with melting points below 100°C are categorised as ionic liquids (ILs). Ionic liquids capable of self-assembling into thermodynamically stable liquid-crystalline phases, on cooling from the isotropic state, are referred to as ionic liquid crystals (ILCs) [1–3]. Thermotropic mesogenic materials, consisting solely of cations and anions, have the typical properties of ionic liquids, as well as nano-scale structures of liquid crystals (LCs), where high degrees of molecular translational and rotational mobilities are combined with partial orientational and positional orders. This synergy results in unique combination of conductivity of ionic liquids and the anisotropic physicochemical properties of liquid crystalline materials. ILCs exhibit rich mesomorphism. Typically, layered (smectic), columnar, and cubic (bicontinuous optically isotropic) phases are formed by ionic mesogens, while least-ordered, nematic phases are uncommon. The presence of macroscopic molecular orientational and spatial ordering in fluid ionic phases leads to new dynamic properties exploited, for example, in the development of functional materials for low dimensional transport of electrons, ions, and molecules in electrochemical energy conversion and storage technologies [4]. For these applications, understanding the molecular/ion transport and dynamics is essential. Besides, there is also fundamental interest in

CONTACT Sergey V. Dvinskikh sergeid@kth.se

understanding complex molecular dynamics in nano-assembled ionic structures.

Translation dynamics by self-diffusion processes are most directly investigated by nuclear magnetic resonance (NMR) spectroscopy combined with pulsed magnetic field gradient (PFG) methods. This technique has been widely used in studying lyotropic and thermotropic mesophases [5–8]. A variety of other experimental approaches have also been applied, including EPR with spin-labelled probes [9], radioactive tracer method [10], optical microscopy of dyes [11], and quasi-elastic neutron scattering [12]; however, none of these methods has gained wide acceptance due to experimental or technical limitations. Moreover, these approaches often yield only indirect estimates of the diffusion coefficients of the molecules constituting the mesophases. The NMR-based methodology is molecular-selective and requires neither foreign probes nor modification of the LC properties. Molecular positions and displacements are encoded by the NMR frequency, which becomes spatially dependent in the presence of a magnetic field gradient [13–16]. A large anisotropy of diamagnetic susceptibility of mesogenic functional groups can induce macroscopic molecular alignment in the presence of the strong magnetic field of an NMR spectrometer. This provides access to diffusion anisotropy.

Extensive reviews on ionic mesogen design, synthesis, characterisation, and application of ILCs were published recently [1–4]. The present article aims to review the reports on molecular/ion self-diffusion in ILCs. This review can be considered as an update to the review on diffusion in thermotropic LCs published in 2006 [7], but focuses exclusively on ILCs. A part of discussion is devoted to the NMR diffusion methodology in LCs and is presented in the next section, where basic and advanced techniques are introduced. The results of employing NMR to determine the components of the diffusion tensor in ionic mesophases are given thereafter. Starting by presenting a new, original diffusion study of a smectic phase of an imidazolium-based mesogen, investigations of smectic, columnar, and cubic phases are reviewed.

2. NMR methods for diffusion studies of liquid crystals

2.1. Field-gradient NMR

In diffusion NMR experiments, the displacements of molecules are detected via field-gradient-assisted de- and re-phasing of spin coherences. In the absence of translational motion, spin magnetization, de-phased during the *encoding* period, is fully recovered after re-phasing during the *decoding* period. Random molecular displacements induce re-phasing errors, leading to decreased magnetization upon increasing the de-phasing efficiency. Residual magnetization is recorded in the form of spin echo signals (Figure 1). In isotropic liquids, the echo amplitude is given by the Stejskal-Tanner relation [13]:

$$I \propto \mathrm{e}^{-(\gamma g \delta)^2(\Delta-\delta/3)D} = \mathrm{e}^{-bD} \qquad (1)$$

where g and δ are the strength and the length of the applied gradients, respectively; Δ, the diffusion time; D, the self-diffusion coefficient; γ, the gyromagnetic ratio of the observed nuclei; $b = (\gamma g \delta)^2(\Delta - \delta/3)$. The effect of the anisotropic diffusion, characterised by diffusion tensor **D**, is described by replacing the term g^2D in Equation (1) with **gDg**. In conventional diffusion experiments employing gradient pulses, the signal intensities are recorded on increasing the gradient

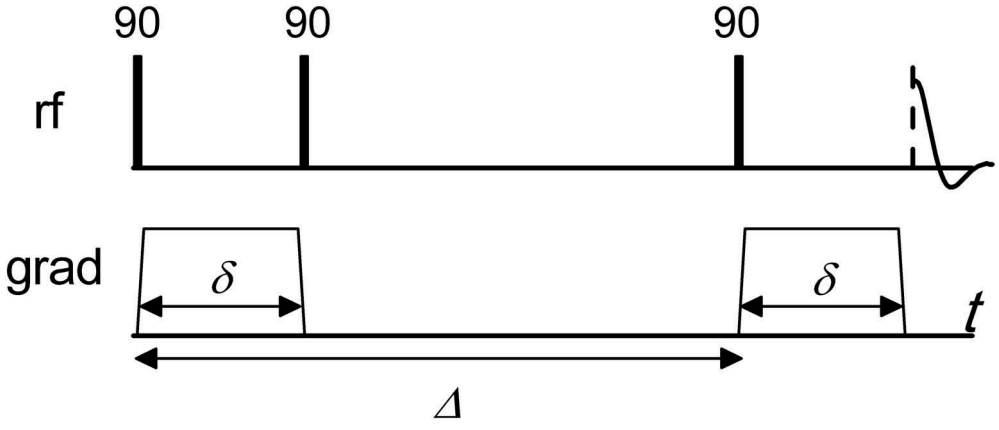

Figure 1. Pulse sequence for pulsed-field-gradient stimulated spin echo NMR experiments. Radio-frequency (rf) 90-degree pulses and gradient pulses (grad) are shown on upper and lower panel, respectively. δ is the length of the gradient pulse, and Δ is the time delay between the gradient pulses.

strength, g, and the diffusion coefficient, D, is calculated by fitting Equation (1) to experimental points.

In practice, the basic stimulated echo sequence represented in Figure 1 is expanded with various blocks to suppress possible experimental artefacts. The influence of convectional flow, induced at elevated temperatures, is diminished by employing a double stimulated echo sequence [17]. The effect of eddy currents, after field gradient pulses, can be suppressed by a longitudinal eddy current delay block [18]. The artefacts due to cross-relaxation are removed by applying bipolar gradient pulses [19].

Diffusion can be measured only if the spin magnetization de-phasing is significant. This can be considerably limited in LCs. The anisotropic spin interactions in LCs lead to spectral splitting and line-broadening as well as correspondingly quick decays of spin coherences. The signal loss due to spin-spin relaxation process, limits the gradient encoding/decoding times (gradient pulse length δ in Figure 1), and thereby places a lower limit on the assessable diffusion coefficients [20].

2.2. PFG NMR with spin decoupling

Line broadening and splitting effects for abundant spins $I = 1/2$ in LCs are, in most cases, significant due to homonuclear dipolar interactions. The strategy explored for the diffusion experiment in samples with dipolar-broadened spectra involves the suppression of the homonuclear spin coupling by appropriate radio-frequency (rf) pulse sequences. Dipolar decoupling is, however, inefficient if the rf pulses are applied in the presence of a large frequency offset induced by the field gradient. In this context, the advantage of the magic-echo (ME) homonuclear decoupling pulse sequence is the relatively long windows between the rf pulses, where gradient pulses can be inserted; thus, off-resonance effects are avoided (Figure 2) [21,22]. ME-PFG has been the conventional approach for investigating the diffusion in non-ionic LCs [7,22–27] and also, recently, in ILCs [28]. Other methods based on dipolar decoupling have been described, where the frequency offset effects are diminished by limiting the active sample volume using slice selection methods [29,30]. This strategy, however, suffered from decreased signal intensities and a relatively low gradient encoding efficiency.

2.3. Stray-field NMR

To achieve sufficient spin-coherence diffusional de-phasing, stronger field gradients can be used as an alternative to the suppression of line broadening. Experiments on LCs have been performed using large static gradients in the stray field of conventional superconducting NMR magnets [20,31,32]. The experimental pulse sequence is as in Figure 1, but with the field gradient field constantly present. The disadvantage of this approach is the large broadening of the recorded signals, owing to the static gradient present during detection, leading to a decrease in the signal-to-noise ratio. Furthermore, the limited excitation range of the rf pulses in the presence of a large frequency offset contributes to the signal loss. Moreover, the gradient strength and direction cannot easily be varied.

2.4. NMR relaxation

The diffusion coefficients in the mesophases were also obtained from the T_1 relaxation time measurements [33–35]. Estimation of the diffusion coefficients from

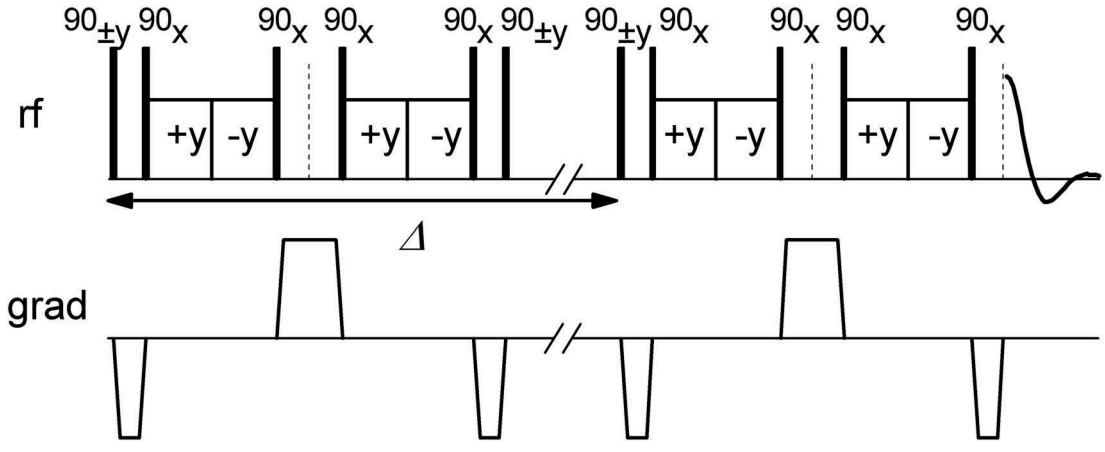

Figure 2. Stimulated echo sequence combined with magic-echo decoupling for measuring the diffusion coefficients in the presence of static dipole-dipole interactions [7]. Gradient pulses are inserted into the windows of the decoupling sequence.

the relaxation rate requires the separation of contributions from a number of molecular processes, such as individual and collective reorientation modes. Therefore, the relaxation measurements were performed in a wide Larmor frequency range by field-cycling NMR [33]. In this technique, which employs electromagnets, the magnetic field is fast switched between different levels, and the Larmor frequency can be varied in the kHz to tens of MHz wide range. The diffusion coefficients extracted from the relaxation data characterise the translational motion on the molecular length-scale, in contrast with the micrometre-scale diffusion coefficients obtained by the field-gradient techniques. A significant number of field-cycling NMR studies on conventional LCs [36] and non-mesogenic ionic liquids have been reported [37]; however, no applications of this method to ILCs have been published.

2.5. Anisotropic diffusion and director alignment

Translational diffusion in liquid crystals is represented by a second-rank diffusion tensor that is diagonal in the director reference frame. In LCs with cylindrical symmetry, only two principal components of the diffusion tensor are independent. Conventionally, coefficients $D_{||}$ and $D_{\perp}$ are defined for diffusion along and perpendicular to the director, respectively. To characterise the diffusion tensor, experiments performed at several gradient orientations, relative to the director, are required. The orientation of the director in the sample can be homogeneous or randomly distributed with respect to the direction of the external magnetic field and field gradient.

Many LCs, when exposed to a strong magnetic field, exhibit homogeneous or partial director alignment. Low viscous LCs (for example, nematics) align spontaneously under magnetic field exposure, while for some other phases the alignment can be obtained by slow cooling from an isotropic or intermediate nematic phase. Depending on the sign of the molecular magnetic susceptibility anisotropy, $\Delta\chi$, a director alignment parallel or perpendicular to the external magnetic field vector is induced. Although $\Delta\chi$ is relatively small, the collective effect in a bulk sample is sufficient to overcome thermal fluctuations. In a homogeneously oriented sample, $D_{||}$ and $D_{\perp}$ can be measured using orthogonal gradient coils. Macroscopically oriented LCs are contrasted to 'powder'-like samples, where the orientation of the director varies randomly across the sample.

The diffusional decay recorded in the experiments on partly- or un-aligned samples, becomes a composite decay due to different director orientations to the applied field gradient. For a sample region, where the director is aligned at angle θ to the gradient, the relevant diffusion coefficient is a combination of $D_{||}$ and $D_{\perp}$ [38,39].

$$D(\theta) = D_{||}\cos^2\theta + D_{\perp}\sin^2\theta.$$

For a 3D powder distribution, by averaging over all solid angles, the echo decay is given by [38]:

$$I \propto \mathrm{e}^{-bD_{\perp}} \int_0^{\pi/2} \mathrm{e}^{-b(D_{||}-D_{\perp})\cos^2\theta} \sin\theta d\theta \qquad (2)$$

If the sample is a '2D powder' with directors distributed perpendicularly to the z axis, the echo decay for the gradient along x (or y) axis is described by the expression [39],

$$I \propto \mathrm{e}^{-bD_{\perp}} \int_0^{\pi/2} \mathrm{e}^{-b(D_{||}-D_{\perp})\cos^2\theta} d\theta \qquad (3)$$

Since the director aligned in xy-plane makes a 90° angle to the z-axis (symmetry axis) for any location within the sample, the signal decay with the gradient in the z direction is given by Equation (1), with $D = D_{\perp}$.

If other effects such as restricted diffusion [16] do not complicate the decay, the diffusion components can be obtained from the analysis of the composite decay by fitting data points to Equations 2 and 3. The effect of restricted diffusion can be recognised by comparing the decays at different diffusion times. The accuracy of extracting diffusion coefficients from the composite decay can be limited due to deconvolution errors, particularly when the values are within the same order of magnitude.

In a limiting case, with the LC director oriented randomly on the diffusion length scale (small domain size limit), the exponential decay of Equation (1) is resulted with the average diffusion coefficient. For a 3D powder, the diffusion coefficient is $\langle D\rangle = (D_{||} + 2D_{\perp})/3$, and two components cannot be independently extracted. For a 2D distribution, the diffusion coefficient in the transverse plane is $\langle D\rangle = (D_{||} + D_{\perp})/2$, while diffusion along the symmetry axis is not affected: $D_z = D_{\perp}$ [40].

To illustrate these different scenarios, diffusion decays are calculated and plotted in Figure 3 for particular combinations of diffusion coefficients, $D_{\perp}/D_{||} = 4$ and $D_{\perp}/D_{||} = 1/4$. The characteristic curvature of the semi-logarithmic plot of echo intensity log(I) versus $b = (\gamma g\delta)^2(\Delta - \delta/3)$ is observed for the decays given by Equations 2 and 3.

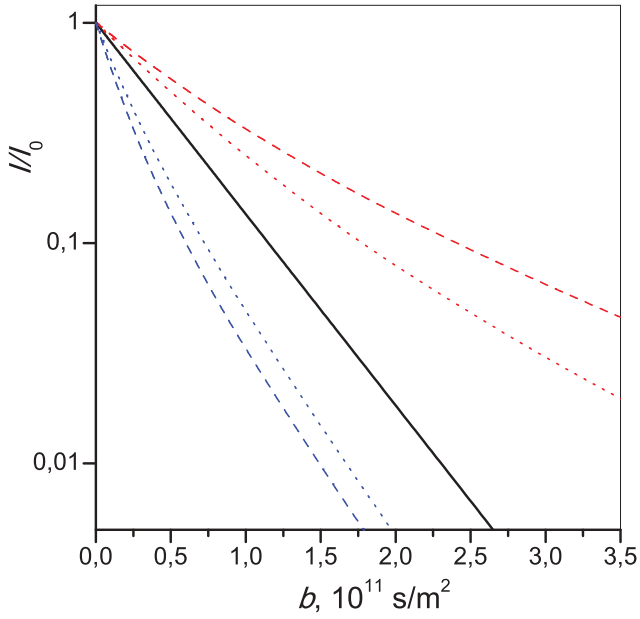

Figure 3. (Colour online) Diffusional decays of the echo signals calculated for isotropic diffusion (solid black line) and composite diffusion for 3D (dotted lines) and 2D (dashed lines) powders, calculated according to Equations 2 and 3, with $D_{\perp}/D_{\parallel} = 4$ (red lines) and $D_{\perp}/D_{\parallel} = 1/4$ (blue lines).

3. Experimental studies of diffusion in ionic liquid crystals

3.1. Smectic layered phase

A wide variety of ionic mesogen structures have been reported, the majority of which are built from a positively charged head group linked to a long aliphatic chain. This structure favours the formation of smectic phases induced by phase segregation of incompatible, charged and hydrophobic, moieties. Electrostatic cation-anion interactions contribute to the stabilisation of layered structures, which can be formed with relatively low molecular orientational order as compared to that in their non-ionic counterparts [41,42]. The most extensively studied ILCs are based on imidazolium cation. Reduced ionic interaction due to charge delocalization in the aromatic core promotes low transition temperatures in these materials, thereby increasing their application potential. NMR diffusion studies of imidazolium based ILCs, exhibiting smectic A phases, have been reported [28,43]. Investigating organic cation diffusion requires the application of spin-decoupling-based methods. The diffusion of small and symmetric counter-ions, if bearing suitable spins, usually fluorine-19 or lithium-7, can be studied by conventional spin-echo field-gradient methods.

In the next section, the diffusion study of hydrated 1-dodecyl-3-methyl-imidazolium chloride (C_{12}mimCl) ionic liquid, exhibiting a smectic A phase, is presented in details. Thereafter, literature reports on diffusion in ionic smectic phases are reviewed.

3.1.1. Diffusion in a smectic a phase of a hydrated C_{12}mimCl

The thermal behaviour of ILCs with hydroscopic counter-ions can be influenced by hydrogen bonding between anion and water. Partly hydrated samples of imidazolium-based ionic liquid crystals with Cl^- counter-ions had significant water-content effects on the stabilisation of the smectic mesophase [44–46]. Here, we present the diffusion study of hydrated C_{12}mimCl and compare our data to the results obtained in a previous study on a dehydrated sample [28].

The C_{12}mimCl sample purchased from ABCR GmbH, Karlsruhe, contained negligible water amount of ~0.02 wt% (estimated from ^{1}H NMR spectra in the isotropic phase). The sample formed a smectic A phase in the temperature range of 45–120°C. A partly hydrated sample with 5.5 wt% of H_2O (or 87 mol%) was obtained by equilibrating for 48 h in a desiccator with 85% relative humidity, stabilised by a saturated KCl solution. The hydrated sample exhibited a significantly wider smectic phase range of 30–160°C.

About 300 mg of the sample was sealed in a 5 mm NMR tube. The measurements were performed on a Bruker 500 Avance II spectrometer at a Larmor frequency of 500 MHz, using a microimaging probe with 3-directional gradients of maximum strength 2.8 T/m. The stability of the hydration level during the diffusion measurement was confirmed by inspecting the ^{1}H NMR water signal intensity in the isotropic phase prior and after completing the diffusion experiments.

The diffusion in the isotropic phase was measured using a standard double-stimulated-echo pulse sequence which compensates for the effects of convectional flow [17]. The diffusion measurements in the smectic phase were performed in the sample prepared by cooling from the isotropic phase under exposure to a magnetic field of 11.7 T of the spectrometer, at a slow cooling rate of <1°C/min. Interestingly, the director alignment in the sample can be obtained, also, at a relatively fast cooling rate of >10°C/min, as was already reported for similar ILCs [43]. This is in contrast to non-ionic smectics, which are prepared aligned either in intermediate nematic phase or by slow cooling from the isotropic state [24,47]. The sample alignment with the director distributed in the plane perpendicular to the magnetic field was confirmed by recording an ^{13}C NMR spectra [42]. The ^{1}H NMR spectra in the mesophase displayed a dipolar-broadened line of about 8 kHz wide and correspondingly short spin-spin relaxation time below 100 μs. This line width is smaller than that typically observed in non-ionic thermotropic phases; however, it is still too broad for diffusion measurements by conventional PFG NMR. Therefore, the ME-PFG method was applied.

Faster diffusion was found along the magnetic field. In the aligned sample, the smectic layers are parallel to the z direction. Therefore, the diffusion in this direction reports on molecular displacement within the smectic layers and the experiment thus provides a direct estimate of the diffusion coefficient perpendicular to the phase director, $D_{\perp}$. In contrast, the diffusion in the presence of an x gradient is contributed by the displacements both parallel and perpendicular to the director because of the random director distribution in the xy-plane (2D powder). Therefore, composite decay is recorded. The diffusion coefficient along director $D_{||}$ is obtained by performing a fit of experimental points to Equation 3. As discussed above, this model is valid in the limit of a large domain size, $L > (2D\Delta)^{1/2}$, compared to the diffusion path length. The decays measured at different delays, Δ, exhibited no significant variation, thus confirming this assumption.

The temperature dependencies of the diffusion coefficients in the isotropic and smectic A phases are shown in Figure 4. Diffusion is much faster compared to the diffusion in the dehydrated sample reported in [28]; activation energies are slightly lower. Interestingly, the diffusion anisotropy in the mesophase is considerably larger in the hydrated sample, $D_{\perp}/D_{||} \approx 7$–$9$, versus 4–5 in anhydrous material [28]. Profound hydration effects on stability and range of the mesophase have been previously reported for a number of mesogenic halide salts [1,44–46]. Herein, we report, for the first time, a dramatic diffusion acceleration upon sample hydration. Furthermore, the diffusion

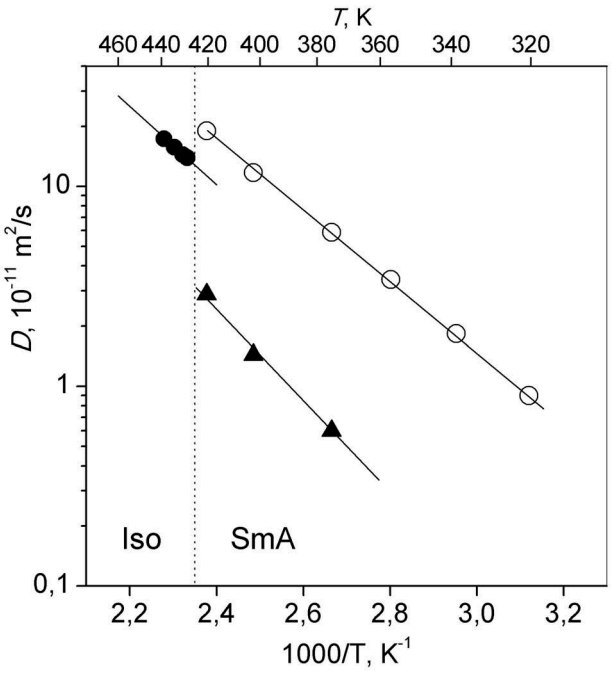

Figure 4. Cation diffusion coefficients, D_{iso} (●), $D_{||}$ (▲), and $D_{\perp}$ (o) in the isotropic and smectic A phases of C_{12}mimCl ionic liquid. Lines are guides for the eye.

anisotropy increases. Hence, water promotes diffusion within the layers to a larger extent compared to that in the perpendicular direction. In smectic ILCs, the dominant layer-stabilising effect is due to a 'charge-ordered' nanoscale segregation induced by ionic interactions, while the orientational ordering is less important [1,41,48,49]. Water molecules contribute further to the structure stabilisation by the formation of a hydrogen bonding network in the ionic sub-layers [1].

3.1.2. Diffusion in C_{12}mimBF$_4$ and C_{12}mimCl

Cifelli et al. performed pulsed-field-gradient NMR measurements and compared the anisotropic diffusion of cations and anions in smectic ILC C_{12}mimBF$_4$ [28]. For cation diffusion in the smectic phase, the ME-PFG method was used to suppress proton homonuclear couplings. ^{19}F NMR was exploited to measure the diffusion of BF_4^- ions. Since ^{19}F NMR spectrum exhibited a narrow spectral line, a standard spin-echo sequence was used.

For both cations and anions, diffusion was faster in the direction perpendicular to the director (Figure 5). Moreover, for the anions, the diffusion is faster, while the diffusion anisotropy $D_{\perp}/D_{||}$ is smaller, ≈1.2, compared to ≈1.8 for the cations. This suggests a separation of the ionic pairs; the smaller and symmetric anion moves faster in the smectic layered structure. Cations, having anisotropic shapes and large sizes, also

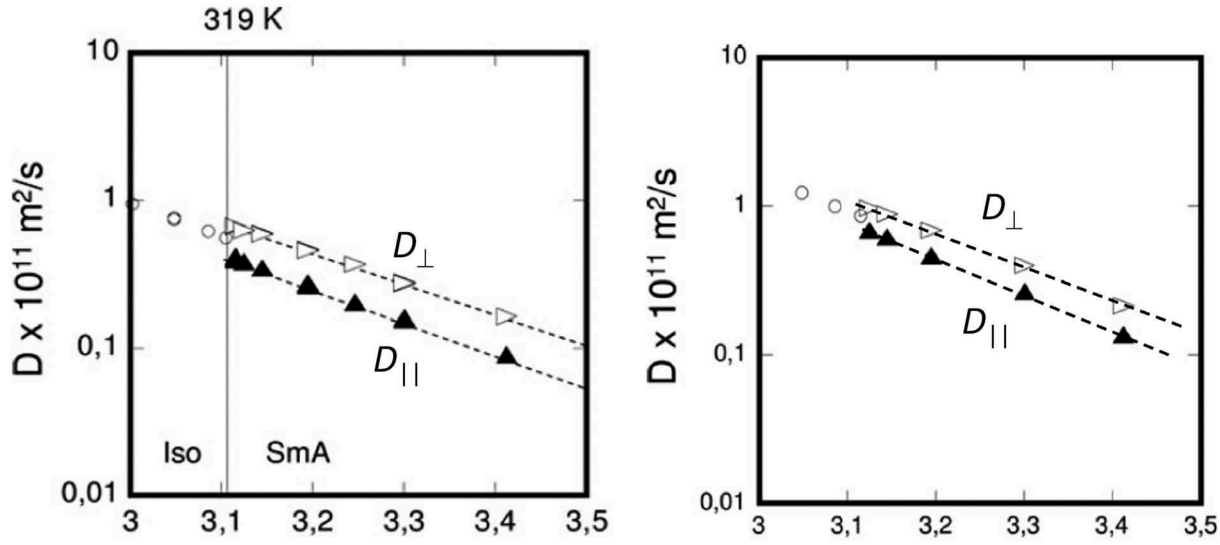

Figure 5. Diffusional coefficients of C_{12}mim cations (left) and BF_4 anions (right) in isotropic and smectic A phases of $C_{12}mimBF_4$ ionic liquid [28]. Adapted with permission from Cifelli et al: Study of Translational Diffusion Anisotropy of Ionic Smectogens by NMR Diffusometry. Mol Cryst Liq Cryst. 2015;614:30–38. Copyright 2015 Taylor & Francis.

experience van der Waals interactions with neighbours in addition to electrostatic interactions with anions.

In the same study, diffusion was compared for smectic ILCs having the same mesogenic cation and different anions [28]. A much higher anisotropy $D_{\perp}/D_{||}$ of cation diffusion, 4.2, was found in C_{12}mimCl sample compared to that in $C_{12}mimBF_4$, 1.8; further, at comparable temperatures, diffusion is slower for C_{12}mimCl mesogen. The mesophase stability is influenced by the type of anions, and it reflects the ability of the anion to build an extended network with charged imidazolium headgroups. For example, for the same imidazolium-based materials, mesophase stability decreases when Cl^- is replaced with BF_4^-, owing to the decreased interactions (electrostatic attraction, hydrogen bonding) between the cation and anion [1]. This trend can explain the significant difference in the observed diffusion anisotropy in these two materials. Indeed, more constrained displacement of the molecules between the layers and faster diffusion within the layer better defines the layered structure of the mesophase.

A similar diffusion trend is expected for anions. However, diffusion measurement by NMR of chlorine was precluded by a high quadrupolar coupling and a low gamma ratio of chlorine spins.

3.1.3. $C_n$mimBF_4 and $C_n$vimBF_4 mixtures with $LiBF_4$

Diffusion has been studied in smectic A phases of pure ionic liquids, $C_n$mimBF_4 and $C_n$vimBF_4, and their mixtures with $LiBF_4$ salt (n = 14, 16, mim – methylimidizalium, vim – vinylimidazolium) [43]. The authors noted easy alignment of the smectic layers under the magnetic field upon cooling from the isotropic phase even at fast cooling rates. The domain size, that is, the persistence length of the director orientation, is known to be dependent on the preparation condition, particularly on the cooling speed and other factors, such as sample purity. Domain sizes on the μm scale can have an influence on the measured diffusion, as discussed above in the Methodology section. The diffusion results in the work [43] were analysed assuming a small domain size and monoexponential diffusion decays.

Only diffusion of small ionic species, BF_4^- and Li^+, by ^{19}F and ^7Li PFG NMR, respectively, were studied, while the diffusion of the organic cations was not measured due to instrument limitations. For BF_4^-, the diffusion along the magnetic field, i.e. perpendicular to the phase director, was measured, while for Li^+, the diffusion was measured in two orthogonal directions. (Note, in work [43] the opposite notations for $D_{||}$ and $D_{\perp}$ were used compared to those introduced in Section 2)

When the C_{14}vimBF_4 ionic liquid was mixed with 0.3M $LiBF_4$, the diffusion coefficient of the BF_4 anion decreased by a factor in the range of 2 to 4. This was explained by the hindered ionic mobility with increased concentration of polar moieties. Li diffusion displayed significant anisotropy ratio up to 1.8. This is close to a factor of 2 expected for a 2D powder with a domain size smaller than the diffusion path length, $L < (2D\Delta)^{1/2}$ (and assuming negligible diffusion along the director).

The diffusion in samples with different organic cations (C_{14}vim and C_{16}vim, and C_{14}vim and C_{14}mim) was analysed in terms of the cationic transference number, $T_{cation} = D_{cation}/(D_{cation}+D_{anion})$. This value was insensitive to

the chain length, while it decreased when the vinyl group was changed to methyl group in the imidazolium core. This further confirmed the segregation of apolar and ionic moieties as a major factor contributing to the self-assembly of the smectic layers.

3.2. Columnar phase

Yoshio et al. prepared disc-shaped supramolecular mesogens via self-assembly of fan-shaped tris-(alkyloxy)phenylene molecules, functionalised with an imidazolium salt. These discotic structures, in turn, aggregate into a columnar phase, where the imidazolium moiety forms a 1D ionic path inside the columns [50]. Such materials were shown to display relatively high conductivities along the columnar axis rather than perpendicular to it. Frise et al. studied the diffusion in the hexagonal columnar and the isotropic phases of such salts with a PF_6^- anion [51]. The sample in the columnar phase was macroscopically aligned under exposure to the magnetic field. The orientation of the phase was tested by ^{2}H NMR of the probe molecules which confirmed that the director (average direction of column axes) is distributed in the plane orthogonal to the magnetic field (2D powder distribution).

Studies were conducted by conventional spin-echo diffusion NMR experiments. For the diffusion measurements of the organic cation, the proton signal of the methyl groups was exploited, which in this sample, exhibited a relatively long spin relaxation $T_2 > 1$ ms. For measuring the diffusion of PF_6^-, ^{19}F NMR was applied.

In the aligned sample, with the columnar axes distributed in the *xy*-plane, the diffusion decay with *z* gradient reported on the diffusion coefficient perpendicular to the phase director, $D_\perp$. Conversely, the diffusion in the presence of *x* (or *y*) gradient was contributed by the displacements both parallel and perpendicular to the director. The resulting composite decay was analysed to obtain diffusion coefficient $D_{||}$, while $D_\perp$ was set to the value obtained from the experiment with the *z*-gradient. By performing measurements at different diffusion times, Δ, it was verified that the large domain size limit, $L > (2D\Delta)^{1/2}$, is valid; thus, the diffusion anisotropies *within* individual domains were observed.

The authors found that the PF_6 anion diffusion in the mesophase was faster along the columnar axis and the diffusion anisotropy, $D_{||}/D_\perp$, was ≈ 5. In contrast, for the imidazolium cation, the anisotropy was negligible, $D_{||} \approx D_\perp$. Faster anion diffusion along the columnar axis and slower diffusion perpendicular to the columns, as compared to the case with cation diffusion, validated the ion channel model of the columnar ionic mesophase. In addition, ion dissociation in the mesophase was confirmed, while in the isotropic phase of this material, the very similar diffusion coefficients of two species suggested significant ion pairing.

3.3 Cubic phase

Optically isotropic mesophases of cubic symmetry are relatively rare for thermotropic ILCs. In multi-continuous ionic cubic phases, periodic interpenetrating molecular/ion 3D network is formed with a long-range positional order. Such phases show potential as charge-transporting materials in molecular electronics. Polymerisable quaternary ammonium salts, forming bicontinuous cubic phases, were used for the preparation of ion-conductive films with 3D-interconnected ion channels [52].

A high molecular mobility (translational and rotational) within the 3D isotropic structure of the cubic mesophase leads to efficient averaging of the anisotropic spin interactions. Thus, the NMR spectra exhibit relatively narrow lines and correspondingly long spin-spin relaxation times for both anions and cations. Therefore, the standard stimulated-echo PFG technique can be applied to measure diffusion coefficients in cubic phases.

Frise et al. studied self-diffusion in the bicontinuous cubic phase of a fan-shaped ammonium tetrafluoroborate salt [53]. In their study, nanoscale segregation of incompatible moieties led to the formation of highly ordered interconnected ion-channel networks, which facilitated anion transport. The cation and anion diffusion coefficients were distinctly measured via ^{1}H and ^{19}F NMR, respectively. The convection artefacts, at high temperatures, were diminished by employing a double stimulated echo sequence [17]. The artefacts due to cross-relaxation were removed by applying bipolar gradient pulses [19]. The authors considered that, for the sample prepared by sufficiently slow cooling from the isotropic phase, the domain boundaries had no significant effect on the diffusion measurements.

A significant difference in the diffusion for the two ionic species in the cubic phase was found, while in the isotropic phase, the diffusion coefficients were similar. The comparable diffusion of anions and cations, in spite of the large difference in their sizes, was explained by strong ion pairing, where the diffusion is controlled by the displacement of the relatively large ion. In contrast, in the mesophase, where anions diffused about twice as fast as cations, ion pairs were dissociated. The

authors suggested that the ion pair dissociation might explain the much higher ionic conductivity observed in the cubic phase, compared to that in the isotropic state [54]. The diffusion results were consistent with the ionic nano-channel network model of the ionic cubic phase.

Conclusions

The translational diffusion coefficients of molecules/ions in ILCs can be accurately measured by pulsed-field-gradient NMR. The methodology is applied to samples with natural isotopic abundance, and it requires no foreign probes. Since it is also molecular selective, the diffusion coefficients of different ionic species can be distinctly measured. Proton NMR was applied to measure the diffusion of organic cations. Conventional NMR spin-echo methods can be used in optically isotropic mesophases (cubic), while in most other cases, PFG NMR combined with spin-decoupling was required. The diffusions of small and symmetric inorganic counter-ions containing NMR sensitive spins, such as ^{19}F and ^{7}Li, were measured by conventional PFG sequences.

Diffusion anisotropy is most easily accessed if a mesophase sample is macroscopically aligned. The anisotropic diamagnetic susceptibility of mesogenic functional groups induces a macroscopic molecular alignment in the presence of a strong magnetic field of NMR spectrometer. This provides access to the diffusion anisotropy by applying gradients in orthogonal directions. If the director alignment is random (2D or 3D distribution) along the field gradient direction, a relatively large domain size exceeding a spatial range, over which diffusion is measured, is preferred to accurately extract the diffusion tensor components. A larger domain size is obtained with a slow sample-cooling rate from the isotropic phase.

Anisotropic diffusion was observed in the smectic and columnar phases. Diffusion was found to be faster within the aggregates, layers or columns, compared to the diffusion across the aggregates. The anisotropy varied with the type of anion: a relatively small anisotropy was found for the decreased interactions (electrostatic attraction, hydrogen bonding) between the cation and anion. A strong hydration effect on the diffusion anisotropy, which was related to the water contribution to the hydrogen-bonding network in the ionic sublayers, was observed. The diffusion temperature dependencies were well described by the Arrhenius law. The activation energies were similar for the two diffusional components and for the diffusion coefficients in the isotropic phase. Furthermore, the diffusion coefficients near the phase transition were of the same order of magnitude with the relationship: $D_{within} > D_{iso} > D_{across}$. This general behaviour is consistent with the results of molecular dynamics computational analysis of diffusion in the ionic smectic phase [55].

The domain of nano-structured, ion-conductive mesogenic materials is a rapidly growing research field. Diffusion coefficients deliver direct molecular-level information on translation mobility, and thus contribute to the fundamental understanding of the complex ion dynamics in ionic liquid-crystalline materials. The obtained diffusion data have provided support for structural models in ILCs. Ion diffusion coefficients depend on the extent of ionic association, and thus reflect ionic activity. Advances in understanding molecular/ion diffusion processes assisted the molecular-level explanation of the macroscopic conductivity behaviour in an anisotropic low-dimensional environment.

Disclosure statement

No potential conflict of interest was reported by the author.

Funding

This work was supported by the Swedish Research Council VR and by the Russian Foundation for Basic Research (project no. 17-03-00057).

References

[1] Goossens K, Lava K, Bielawski CW, et al. Ionic liquid crystals: versatile materials. Chem Rev. 2016;116:4643–4807.
[2] Fernandez AA, Kouwer PHJ. Key developments in ionic liquid crystals. Int J Mol Sci. 2016;17:731.
[3] Axenov KV, Laschat S. Thermotropic ionic liquid crystals. Materials. 2011;4:206–259.
[4] Kato T, Yoshio M, Ichikawa T, et al. Transport of ions and electrons in nanostructured liquid crystals. Nat Rev Mater. 2017;2:17001.
[5] Lindblom G, Orädd G. NMR studies of translational diffusion in lyotropic liquid crystals and lipid membranes. Prog Nucl Magn Reson Spectrosc. 1994;26:483–515.
[6] Orädd G, Lindblom G. Lateral diffusion studied by pulsed field gradient NMR on oriented lipid membranes. Magn Reson Chem. 2004;42:123–131.
[7] Dvinskikh SV, Furó I. Nuclear magnetic resonance studies of translational diffusion in thermotropic liquid crystals. Russ Chem Rev. 2006;75:497–506.
[8] Cifelli M, Veracini CA. Translational diffusion in thermotropic smectic phases. Mol Cryst Liq Cryst. 2013;576:127–134.

[9] Moscicki JK, Shin Y-K, Freed JH. Translational diffusion in a smectic-A phase by electron spin resonance imaging: the free-volume model. J Chem Phys. 1993;99:634–649.
[10] Chmielewski AG. Anisotropy of radiotracer diffusion in some nematic liquid-crystals. Mol Cryst Liq Cryst. 1992;212:205–215.
[11] Daoud M, Rais K, Gharbia M, et al. Elliptical diffusion of dye in hexagonal columnar polycatenar mesophases. Liq Cryst. 1999;26:1079–1084.
[12] Belushkin AV, Cook MJ, Frezzato D, et al. A quasi-elastic neutron scattering study of molecular dynamics in a columnar liquid crystal. Mol Phys. 1998;93:593–607.
[13] Stejskal EO, Tanner JE. Spin diffusion measurements: spin echoes in the presence of a time-dependent field gradient. J Chem Phys. 1965;42:288–292.
[14] Stilbs P. Fourier Transform pulsed-gradient spin-echo studies of molecular diffusion. Prog Nucl Magn Reson Spectrosc. 1987;19:1–45.
[15] Callaghan PT. Translational dynamics and magnetic resonance. Oxford: Oxford University Press; 2011.
[16] Price WS. Pulsed-field gradient nuclear magnetic resonance as a tool for studying translational diffusion: part I. Basic theory. Concepts Magn Reson. 1997;9:299–336.
[17] Jerschow A, Muller N. Suppression of convection artifacts in stimulated-echo diffusion experiments. Double-stimulated-echo experiments. J Magn Reson. 1997;125:372–375.
[18] Gibbs SJ, Johnson CS. A PFG NMR experiment for accurate diffusion and flow studies in the presence of eddy currents. J Magn Reson. 1991;93:395–402.
[19] Dvinskikh SV, Furó I. Cross-relaxation effects in stimulated-echo-type PGSE NMR experiments by bipolar and monopolar gradient pulses. J Magn Reson. 2000;146:283–289.
[20] Cifelli M. A practical tutorial to set up NMR diffusometry equipment: application to liquid crystals. Magn Reson Chem. 2014;52:640–648.
[21] Zhang W, Cory DG. First direct measurement of the spin diffusion rate in a homogeneous solid. Phys Rev Lett. 1998;80:1324–1327.
[22] Dvinskikh SV, Furó I, Sandström D, et al. Deuterium stimulated-echo-type PGSE NMR experiments for measuring diffusion: application to a liquid crystal. J Magn Reson. 2001;153:83–91.
[23] Cifelli M, Domenici V, Dvinskikh SV, et al. Translational self-diffusion in the synclinic to anticlinic phases of a ferroelectric liquid crystal. Soft Matter. 2010;6:5999–6003.
[24] Cifelli M, Domenici V, Dvinskikh SV, et al. Translational self-diffusion in the smectic phases of ferroelectric liquid crystals: an overview. Phase Transit. 2012;85:861–871.
[25] Dvinskikh SV, Furo I. Anisotropic self-diffusion in nematic, smectic-A, and reentrant nematic phases. Phys Rev E. 2012;86:031704.
[26] Dvinskikh SV. Pulsed-field-gradient NMR study of anisotropic molecular translational diffusion in nOCB liquid crystals. Appl Magn Reson. 2013;44:169–180.
[27] Cifelli M, Domenici V, Dvinskikh SV, et al. The twist-bend nematic phase: translational self-diffusion and biaxiality studied by ^{1}H nuclear magnetic resonance diffusometry. Liq Cryst. 2017;44:204–218.
[28] Cifelli M, Domenici V, Kharkov BB, et al. Study of translational diffusion anisotropy of ionic smectogens by NMR diffusometry. Mol Cryst Liq Cryst. 2015;614:30–38.
[29] Dvinskikh SV, Sitnikov R, Furó I. ^{13}C PGSE NMR experiment with heteronuclear dipolar decoupling to measure diffusion in liquid crystals and solids. J Magn Reson. 2000;142:102–110.
[30] Dvinskikh SV, Furó I. Combining PGSE NMR with homonuclear dipolar decoupling. J Magn Reson. 2000;144:142–149.
[31] Cifelli M, McDonald PJ, Veracini CA. Translational self diffusion in 4-n-octyloxy-4 ‘-cyanobiphenyl (8OCB) exploited with a static field gradient H-1 NMR diffusometry approach. Phys Chem Chem Phys. 2004;6:4701–4706.
[32] Cifelli M, Veracini CA. Translational self diffusion anisotropy in the smectic A phase measured by a static fringe field gradient H-1 NMR diffusometry approach. Phys Chem Chem Phys. 2005;7:3412–3415.
[33] Noack F. NMR field-cycling spectroscopy - principles and applications. Prog Nucl Magn Reson Spectrosc. 1986;18:171–276.
[34] Terekhov MV, Dvinskikh SV, Privalov AF. A field-cycling NMR study of nematic 4-pentyl-4 ‘-cyanobiphenyl confined in porous glasses. Appl Magn Reson. 1998;15:363–381.
[35] Ferraz A, Figueirinhas JL, Sebastiao PJ, et al. Molecular-dynamics study of the ferroelectric liquid-crystal CLIPNOC by proton spin-lattice relaxation. Liq Cryst. 1993;14:415–426.
[36] Kimmich R, Anoardo E. Field-cycling NMR relaxometry. Prog Nucl Magn Reson Spectrosc. 2004;44:257–320.
[37] Kruk D, Meier R, Rachocki A, et al. Determining diffusion coefficients of ionic liquids by means of field cycling nuclear magnetic resonance relaxometry. J Chem Phys. 2014;140:244509.
[38] Callaghan PT, Jolley KW, Lelievre J. Diffusion of water in the endosperm tissue of wheat grains as studied by pulsed field gradient nuclear magnetic resonance. Biophys J. 1979;28:133–141.
[39] Gaemers S, Bax A. Morphology of three lyotropic liquid crystalline biological NMR media studied by translational diffusion anisotropy. J Am Chem Soc. 2001;123:12343–12352.
[40] Poulos AS, Constantin D, Davidson P, et al. A PGSE-NMR study of molecular self-diffusion in lamellar phases doped with polyoxometalates. J Phys Chem B. 2010;114:220–227.
[41] Saielli G. Fully atomistic simulations of the ionic liquid crystal [C(16)mim][NO_3]: orientational order parameters and voids distribution. J Phys Chem B. 2016;120:2569–2577.
[42] Dai J, Kharkov BB, Dvinskikh SV. Molecular and segmental orientational order in a smectic mesophase of a thermotropic ionic liquid crystal. Crystals. 2019;9:18.
[43] Judeinstein P, Huet S, Lesot P. Multiscale NMR investigation of mesogenic ionic-liquid electrolytes with

strong anisotropic orientational and diffusional behaviour. Rsc Adv. 2013;3:16604–16611.
[44] Bowlas CJ, Bruce DW, Seddon KR. Liquid-crystalline ionic liquids. Chem Commun. 1996:1625–1626.
[45] Bradley AE, Hardacre C, Holbrey JD, et al. Small-angle X-ray scattering studies of liquid crystalline 1-alkyl-3-methylimidazolium salts. Chem Mater. 2002;14:629–635.
[46] Puntus LN, Schenk KJ, Bunzli JCG. Intense near-infrared luminescence of a mesomorphic ionic liquid doped with lanthanide beta-diketonate ternary complexes. Eur J Inorg Chem. 2005;4739–4744.
[47] Dvinskikh SV, Furó I, Zimmermann H, et al. Anisotropic self-diffusion in thermotropic liquid crystals studied by ^{1}H and ^{2}H pulse-field-gradient spin-echo NMR. Phys Rev E. 2002;65:061701.
[48] Ganzenmuller GC, Patey GN. Charge ordering induces a smectic phase in oblate ionic liquid crystals. Phys Rev Lett. 2010;105:137801.
[49] Gorkunov MV, Osipov MA, Kapernaum N, et al. Molecular theory of smectic ordering in liquid crystals with nanoscale segregation of different molecular fragments. Phys Rev E. 2011;84:051704.
[50] Yoshio M, Mukai T, Ohno H, et al. One-dimensional ion transport in self-organized columnar ionic liquids. J Am Chem Soc. 2004;126:994–995.
[51] Frise AE, Dvinskikh SV, Ohno H, et al. Ion channels and anisotropic ion mobility in a liquid-crystalline columnar phase as observed by multinuclear NMR diffusometry. J Phys Chem B. 2010;114:15477–15482.
[52] Ichikawa T, Yoshio M, Hamasaki A, et al. 3D interconnected ionic nano-channels formed in polymer films: self-organization and polymerization of thermotropic bicontinuous cubic liquid crystals. J Am Chem Soc. 2011;133:2163–2169.
[53] Frise AE, Ichikawa T, Yoshio M, et al. Ion conductive behaviour in a confined nanostructure: NMR observation of self-diffusion in a liquid-crystalline bicontinuous cubic phase. Chem Commun. 2010;46:728–730.
[54] Ichikawa T, Yoshio M, Hamasaki A, et al. Self-organization of room-temperature ionic liquids exhibiting liquid-crystalline bicontinuous cubic phases: formation of nano-ion channel networks. J Am Chem Soc. 2007;129:10662–10663.
[55] Saielli G, Voth GA, Wang YT. Diffusion mechanisms in smectic ionic liquid crystals: insights from coarse-grained MD simulations. Soft Matter. 2013;9:5716–5725.